

Modeling of Geothermal Water Cooling System

O. Chahad, A. Refai, K. Ben Mohamed

Faculté des sciences de Tunis, Campus Universitaire, El Manar, Tunis

Ous.chahad@gmail.com

Keywords: Convection, cross flow cooling tower, evaporation, geothermal water, heat and mass transfer, modeling, thermal behavior

ABSTRACT

Cross flow mechanical cooling towers are widely used in the south region of Tunisia for cooling geothermal water in agriculture and domestic ends. These towers are sized empirically and present several problems in regard to operation and electrical energy consumption. The objective of this paper is to study the thermal behavior of this type of cooling towers, through a developed mathematical model, considering the variation of the water mass flow rate inside the tower. The analysis of water and air temperatures distribution along the cooling tower had underlined the negative convection phenomenon at a certain height of the tower. This analysis has shown also that the difference in water temperature between the inlet and the outlet of the tower is much higher than the one of air due to the dominance of the evaporative potential compared to the convective one.

In addition, the variations of the air humidity along the cooling tower and the quantity of evaporated water had been investigated. The loss of water by evaporation is found to be not negligible; in fact it presents 5.1% of the total quantity of water feeding the cooling tower. More effort will be done to decrease this amount due to the lack of water in the south of Tunisia.

1. INTRODUCTION

1.1 Background and Objectives

Tunisia has important low to moderate enthalpy geothermal resources situated mostly in the south part of the country. These resources are used mainly for balneology and for heating greenhouses to boost agricultural production. However, their direct use in irrigation field constitutes a harmful effect on crops growth that requires appropriate water temperature to be maintained. To overcome this constraint, adequate supplies of cooling water are considered in the region for irrigation of agricultural lands.

Different cooling concepts are designed using the two main types: the atmospheric type (i.e. the spiral, cascade, and multiple ponds) and the mechanical draught cooling tower type.

The cross flow mechanical draft cooling towers, considered in this work, represents 32% of the total number of cooling towers operating in the region. They are empirically sized and characterized by a low cooling efficiency, excessive electricity consumption, important loss of water vapor, and the presence of scale on the splash pack.

In this concept, atmospheric air is drawn by the fan from side louvers and moves horizontally through the fill. Geothermal water is uniformly sprayed from nozzles and

distributed over the fill, composed of palm branches, and falls down into the water basin with a gradual decrease in temperature. Figure 1 presents a three-dimensional diagram of a cross flow cooling tower with related geometrical dimensions.

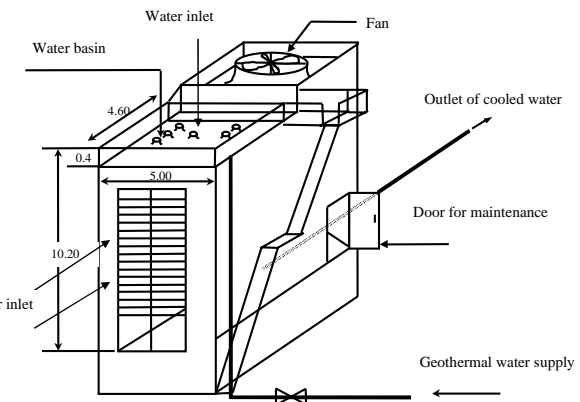


Figure 1: Three-dimensional diagram of cross flow cooling tower

To understand the thermal behavior of the cooling tower and related heat and mass exchanges processes, in order to access to the optimization of the operating conditions, it is required to develop a model for predicting thermal behavior of the cooling system. This model will also be able to predict the quantity of the water loss occurred during the evaporation phase.

This paper aims is to analyze the distribution of water and air temperature inside the cross flow mechanical draft cooling tower as well as the air humidity and to predict the quantity of evaporated water resulting from the cooling process.

1.2 Literature Review

Many authors were interested in the modeling of cooling towers that represents an essential element for the optimization of their operating conditions. Walker et al. (1923) were the firsts to propose a basic theory of cooling towers operating. Coupled transfer of mass and heat had been described by a complex system of differential equations. Although these equations are well known, a serious problem is met in their resolution. The first approach used is to simplify the model by introducing assumptions that decrease the precision of the results. Then, with the apparition of the fast calculators, better precision has been achieved.

Merkel (1925) was the first who presented practical use of the differential equations. In his model, he coupled the heat and mass transfer and assumed a constant water mass flow neglecting the water evaporation rate. It is worth noting that,

the formulation of Merkel is used and discussed by most authors.

Jaber and Webb (1997) applied the theory of conception of heat exchangers on the cooling towers neglecting also the evaporated water rate.

Braun et al. (1989) had modified the relations of thermal efficiency developed in the heat exchanger without evaporation and they assumed a number of Lewis equal to the unit.

El-Dessouky et al. (1997) had developed a modified version of Jaber and Webb's model (Jaber and Webb (1997)). They used an approximate equation for the calculation of the humid air enthalpy. Here, this approximation is too inaccurate to give reliable results.

Bernier (1994 and 1995) had enlightened the performance of a cooling tower while investigating the mechanisms of heat and mass transfer between a droplet of water and the ambient air. In this investigation the author had not considered the variation of the temperature of air crossing the cooling system.

Milosavjevic and Heikkila (2001) studied the thermal performance of a counter current cooling tower considering the evaporation of a quantity of water and assuming that the heat and mass transfer are equivalent to the unit ($Le=1$).

Kaiouani et al. (2004) applied the general model elaborated by Halasz (1998) on a cross flow cooling tower in south Tunisia conditions. This model considers the water mass flow through the tower as a constant value and the varying parameters are water and air temperatures and air humidity.

Most models proposed by previous authors examined the performance of counter flow cooling towers and minor attention is given to cross flow cooling towers where the variation of water mass flow due to evaporation is usually neglected.

2. MATHEMATIC FORMULATION

Convection and evaporation are the two phenomena contributing to the geothermal water cooling process. The directions of water and air flows, levels and sections considered as references in the results presentation are illustrated in Figure 2. The heat and mass transfer equations are solved in a volume element ($\Delta X \Delta Z \Delta y$).

2.1 Equation Development:

At the droplet surface the quantity of water evaporated can be written as:

$$d\dot{m}_w = \frac{\alpha^*}{C_{p,ma}} (\xi_s - \xi_a) dV \quad (1)$$

Where ξ_s is the humidity saturation of air at water temperature and ξ_a is the air humidity in the bulk airflow. α^* is the volumetric heat transfer coefficient.

In the other hand, the same quantity of water evaporated is equal to the airflow multiplied by the air humidity variation.

$$d\dot{m}_w = \dot{m}_a d\xi \quad (2)$$

The total quantity of heat transferred between water and air by convection and evaporation is determined, according to:

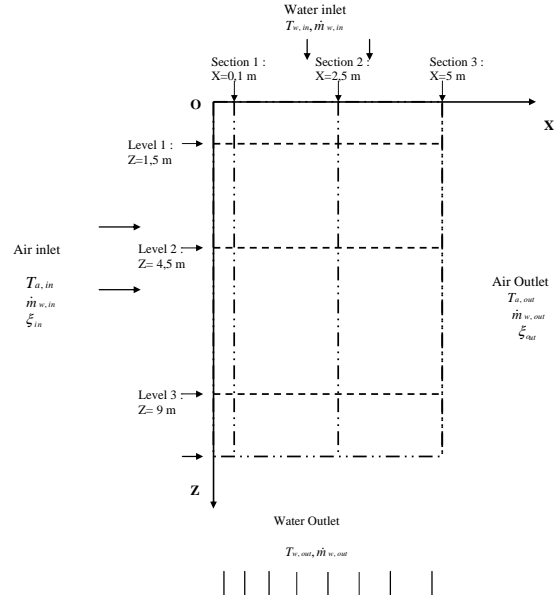


Figure 2: The directions of water and air flows and levels and sections considered as references in the tower

$$dQ_w = \left[\alpha^* (T_w - T_a) + \frac{\alpha^*}{C_{p,ma}} (\xi_s - \xi_a) \Delta h_{ev}(T_w) \right] dV \quad (3)$$

Where $\Delta h_{ev}(T_w)$ is the latent heat of evaporation at water temperature. The heat quantity gained by air can be written as:

$$\begin{aligned} & \left(\frac{\partial \dot{m}_a h_a}{\partial x} \right) dx \\ &= \dot{m}_a \left[(C_{pa} + C_{pv} \xi) \frac{\partial T_a}{\partial x} + (r_0 + C_{pv} T_a) \frac{\partial \xi}{\partial x} \right] dx. \end{aligned} \quad (4)$$

Where r_0 is the latent heat of evaporation of water at 0 °C. The heat quantity lost by water can be written as:

$$\left(\frac{\partial \dot{m}_w h_w}{\partial z} \right) = \left[m_w(z) C_{pw} \frac{\partial T_w}{\partial z} + h_w \frac{\partial \dot{m}_w}{\partial z} \right] dz \quad (5)$$

Since the quantity of heat gained by air is the one lost by water and equal to the quantity of heat transferred between water and air, the following equations can be released:

$$\begin{aligned} & \dot{m}_a \left[(C_{pa} + C_{pv} \xi) \frac{\partial T_a}{\partial x} + (r_0 + C_{pv} T_a) \frac{\partial \xi}{\partial x} \right] dx = \\ & \left[m_w(z) C_{pw} \frac{\partial T_w}{\partial z} + h_w \frac{\partial \dot{m}_w}{\partial z} \right] dz \end{aligned} \quad (6)$$

$$\dot{m}_a \left[(C_{pa} + C_{pv} \xi) \frac{\partial T_a}{\partial x} + (r_0 + C_{pv} T_a) \frac{\partial \xi}{\partial x} \right] dx =$$

$$\left[\alpha^* (T_w - T_a) + \frac{\alpha^*}{C_{p,ma}} (\xi_s - \xi_a) \Delta h_{ev}(T_w) \right] dV \quad (7)$$

2.2 Assumptions

The hypotheses used in the modeling are:

- The process is under steady state
- The distribution of the temperatures and the mass flows of water and air is uniform at the inlet of the cooling tower.
- The specific heat of air, water and steam as well as the heat and mass transfer coefficients are constant.
- The interface of contact between water and air is considerable,
- The volumetric coefficient of heat transfer is high,
- Drops of water are thin; therefore the temperature of water is equal to the one of the interface between water and air,
- Transfers of mass and heat are equivalent, therefore the number of Lewis is equal to the unit,
- The thermal or mass transfer between fluids (air and water) and walls are neglected,
- Operation parameters of the cooling tower are varying only following X and Z directions.

2.3 Diagram of Resolution:

In the simulation, the tower is subdivided into cubic elements of 0.1 m side. The section of an element of volume is presented in figure 3.

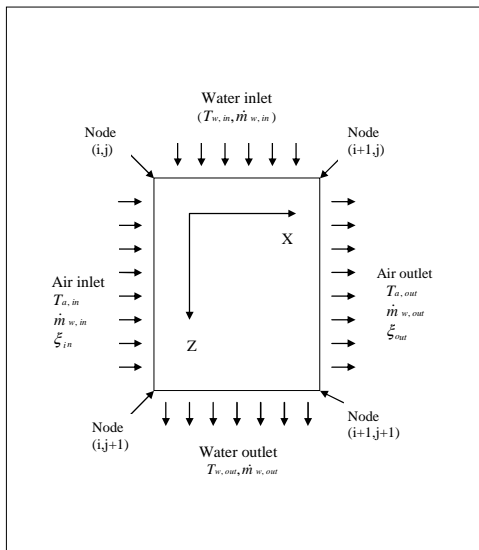


Figure 3: Section of the element volume dV of the cooling tower

The equations system composed of the differential equations (1), (2), (6) and (7) has five unknowns T_a , T_w , ξ , ξ_s , \dot{m}_w .

A relation between ξ_s and T_a can be added to the system according to:

$$P_s = \exp\left(13.765 - \frac{5123}{T_a + 273.15}\right) \quad (8)$$

$$\xi_s = 0.622 \frac{P_s}{P - P_s} \quad (9)$$

The system of equations obtained is not linear; so, the resolution could be performed with Gauss-Seidel's method of iteration. This method consists on assuming an initial guess of the water evaporated quantity at the node (i,j), $\dot{m}_{ev,i,j}$, and then using the rewritten equations (10) and (11) to calculate the water mass flow as well as the absolute humidity of air:

$$\dot{m}_{w,i,j} = \dot{m}_{w,i,j-1} - \dot{m}_{ev,i,j} \quad (10)$$

$$\xi_{i,j} = \xi_{i-1,j} + \frac{\dot{m}_{ev,i,j}}{m_{as}} \quad (11)$$

The water and air temperatures in the node i,j will be determined from the equations (6) and (7). The saturation humidity of air is calculated from the equations (8) and (9), using the derived air temperature value.

Remember, one always uses the most recent guesses to calculate these parameters. It is worth noting, that the new guesses of the $\dot{m}_{ev,i,j}$ is obtained from equation (1). At the end of each iteration, the absolute relative approximate error for each $\dot{m}_{ev,i,j}$ is determined as:

$$|\varepsilon| = \left| \frac{m_{ev,i,j}^{\text{new}} - m_{ev,i,j}^{\text{old}}}{m_{ev,i,j}^{\text{new}}} \right| \times 100 \quad (12)$$

where $\dot{m}_{ev,i,j}^{\text{new}}$ is the recently obtained value of $\dot{m}_{ev,i,j}$, and $\dot{m}_{ev,i,j}^{\text{old}}$ is the previous value of $\dot{m}_{ev,i,j}$.

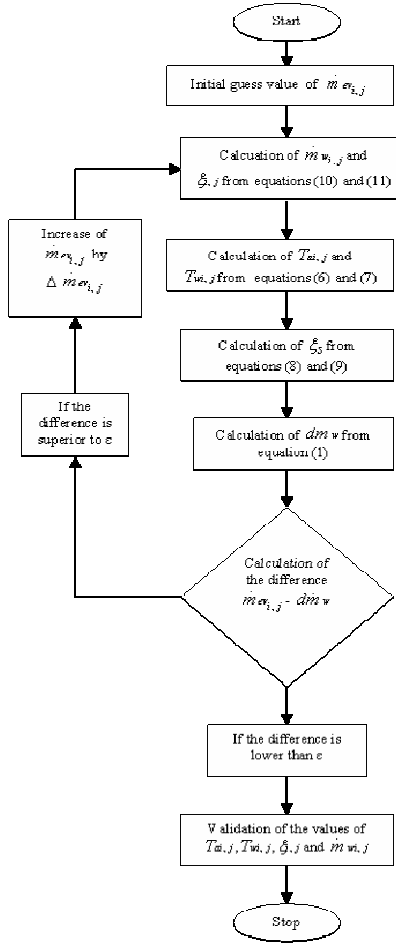


Figure 4: Flowchart showing the main calculation steps of the simulation program

When the absolute relative approximate error for each $\dot{m}_{ev,i,j}$ is less than the prespecified tolerance, the iterations are stopped.

These equations are solved with numerical methods implemented in C++ programming language. The flowchart of calculation is presented in figure 4.

3. RESULTS AND DISCUSSIONS

The general input data are the climatic, operating and iterations parameters. These data are given in Table 1.

Table 1. Input data used in the simulations related to the cross flow mechanical draught cooling tower performances.

Parameters	Values
<u>Climatic Parameters</u>	
Air temperature	38°C
Air relative humidity	15.44%
<u>Operating parameters</u>	
Water temperature	64°C
Water mass flow rate	110 kg/s
Air mass flow rate	224 kg/s
Volumetric coefficient of heat transfer	17,000 W/m ² K
Lewis Number	1
<u>Iteration parameters</u>	
Initial guess values of m_{ev}	10^{-4} kg/s
Step value of m_{ev}	10^{-5} kg/s
Perspecified tolerance	10^{-5}

3.1 Distribution of Water and Air Temperatures Inside the Tower

The variation of the water temperature in the direction of the air flow (OX) is illustrated in figure 5, for the four levels with heights 1.5 m, 4.5 m, 9 m, and 12 m, respectively. This figure shows that the water temperature increases in the direction of air flow (OX). Here, the variation of water temperature is due to the decrease of evaporative and convective potentials.

The air, initially fresh and dry ($X=0$), come across hot water, inducing to a heat and mass transfer. Along its way through the tower, the air temperature and the humidity increase generating a continuous decrease in convective and evaporative potentials that leads to the increase in water temperature between the inlet and the outlet of air.

On level 1, the difference in water temperature between the inlet and the outlet of air is 1°C (figure 5). This difference increases to reach 3°C and 7°C on the second and the third levels, respectively. At the exit of water (level 4), the difference in temperature reaches a value of 10°C.

In the first level, the convective potential between water and the air is significant due to the high temperature of the water. This generated a better heat transfer than the one present in the second level of the tower, where the convective potential is lower. The same explanation is valid for both levels 3 and 4.

Figure 6 illustrates the variation of the air temperature in the flowing direction (OX) at the four levels. It is noticed that after the second level and at a certain height of the cooling tower, the air temperature is decreasing to become lower than water temperature. Here the negative convection is occurred and the water cooling is provoked by evaporation and consequently, water and air are cooled simultaneously. It is worth noting, that the water temperature could be lower than the dry bulb air temperature but could not be, in any case, lower than its wet bulb temperature.

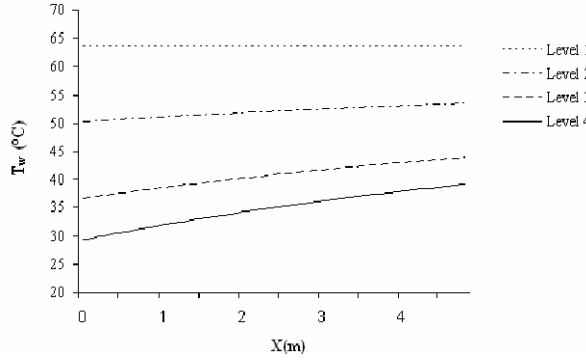


Figure 5: Variation of water temperature through the width of the tower in the direction of (OX) at different levels for $T_a=38^\circ\text{C}$, $T_w=64^\circ\text{C}$, $\varphi=15.44\%$, $m_w=110 \text{ kg/s}$ and $m_a=224 \text{ kg/s}$

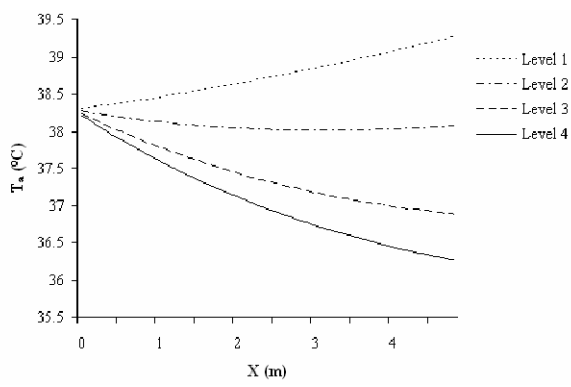


Figure 6: Variation of air temperature through the width of the tower direction of (OX) at different levels for $T_a=38^\circ\text{C}$, $T_w=64^\circ\text{C}$, $\varphi=15.44\%$, $m_w=110 \text{ kg/s}$ and $m_a=224 \text{ kg/s}$

The variation of the air temperature in the direction (OZ) is illustrated in figure 7. This figure shows that along the section 3 and at edge, $X= 5\text{m}$, the variation in air temperature between the top and the bottom of the tower is about 3°C while the variation in the water temperature is approximately 34°C . The supposed reason is that the water cooling along the tower is performed mainly by the evaporation compared to the convective potential.

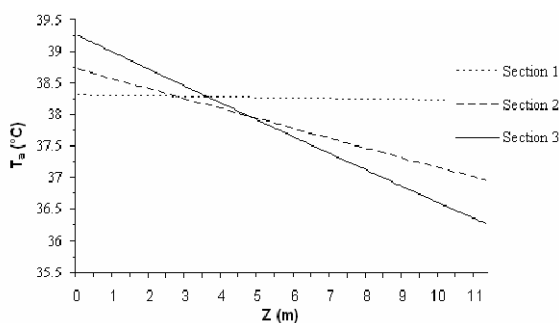


Figure 7: Variation of air temperature through the length of the tower in the direction of (OZ) at different sections water temperature versus z at different sections for $T_a=38^\circ\text{C}$, $T_w=64^\circ\text{C}$, $\varphi=15.44\%$, $m_w=110 \text{ kg/s}$ and $m_a=224 \text{ kg/s}$

3.2 Distribution of the Air Humidity Inside the Tower

The variation of the absolute and saturation humidities of air in the direction (OX) are reported in the figures 8 and 9. These graphs offer the opportunity to understand the air saturation phenomenon inside the cooling tower. As specified previously, the air temperature decreases in his flow direction (OX) on the level 4. This generates the decrease of the saturation humidity (figure 9) while the absolute humidity of the air remains increasing (figure 8). In using the input data for drawing Figure 8 and 9, the saturation state of the air is not achieved since the saturation humidity, $\xi_{s,\min} = 0.04 \text{ kgw/kgas}$, remains largely higher than the absolute humidity of the air, $\xi_{s,\max} = 0.016 \text{ kgw/kgas}$.

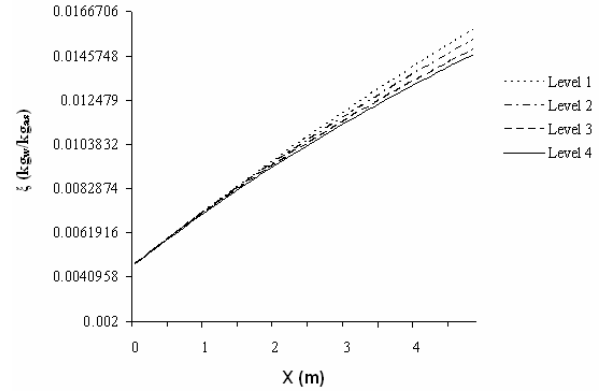


Figure 8: Variation of absolute air humidity through the width of the tower in the direction of (OX) at different levels for $T_a=38^\circ\text{C}$, $T_w=64^\circ\text{C}$, $\varphi=15.44\%$, $m_w=110 \text{ kg/s}$ and $m_a=224 \text{ kg/s}$

However, the saturation phenomenon (the ambient temperature close to the wet bulb temperature) can be attained during the winter climate conditions when the air humidity of the ambient is relatively elevated. This explains the activation of the fog phenomena (due to the intensive evaporation) in the neighborhoods of the cooling tower.

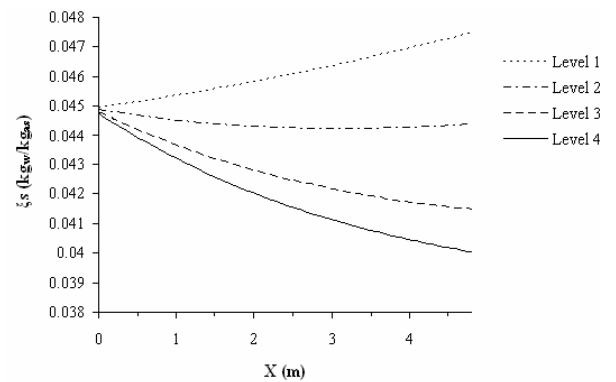


Figure 9: Variation of saturation humidity of air through the width of the tower in the direction of (OX) at different levels for $T_a=38^\circ\text{C}$, $T_w=64^\circ\text{C}$, $\varphi=15.44\%$, $m_w=110 \text{ kg/s}$ and $m_a=224 \text{ kg/s}$

3.3 Distribution of the Evaporated Water Quantity Inside the Tower

Figure 10 shows that the quantity of evaporated water decreases in the tower according to directions (OX) and (OZ). At the level 1, the quantity of evaporated water decreases by $1.3 \cdot 10^{-2} \text{ kgw/kg}$ from $X=0\text{m}$ to $X=5\text{m}$ while at the level 4, it decreases by $2.2 \cdot 10^{-2} \text{ kgw/kg}$. The reduction

in evaporated water quantity \dot{m}_{ev} is inversely proportional to the nearby rate of air humidity. Under the climatic conditions considered in the simulations, and since saturation is not reached, the quantity of evaporated water is significant.

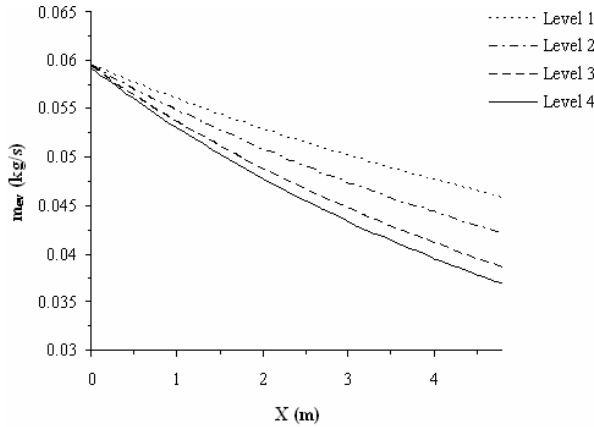


Figure10: Variation in evaporated water quantity through the width of the tower in the direction of (OX) at different levels for $T_a=38^\circ\text{C}$, $T_w=64^\circ\text{C}$, $\varphi=15.44\%$, $m_w=110 \text{ kg/s}$ and $m_a=224 \text{ kg/s}$

The water loss by evaporation is estimated by 5.6 kg/s corresponding to 5.1 % of the quantity of water initially introduced into the cooling tower. This rate is slightly different to that found by Kairouani et al. (2004), i.e. 4%, as this one had used Halasz (1998) assumption neglecting the variation of the water flow in the cooling tower. This result

NOMENCLATURE

C_p	specific heat (J/kg.K)
h	enthalpy (kJ)
L	tower length (m)
Le	Lewis factor
\dot{m}	mass flow rate (kg/m ² .s)
P	pressure (Pa)
r_0	latent heat of evaporation of water at 0 °C (kJ/kg).
T	temperature (°C)
V	volume (m ³)
x, z	Spatial coordinates (m)

Greeks:

α^*	convective heat transfer (W/m ² K)
ζ	absolute humidity (kgw/kgas)
φ	relative humidity of ambient air (%)
ε	absolute error

Subscripts:

a	air
as	dry air
ev	evaporated
i	horizontal position of the node
j	vertical position of the node
ma	moist air
s	saturation
v	vapour
w	water

confirms, also, the limitation of the models presented widely in the literature neglecting the water evaporation. The cumulative quantity of the water loss during one year is estimated by $1.8 \cdot 10^6 \text{ m}^3$. This important water quantity represents the yearly domestic water consumption of about 90.000 inhabitants if we assume that the global water use in domestic sector is $20 \text{ m}^3/\text{person per year}$ (Ayoub et al. (1996))

CONCLUSION

The modeling of the thermal behavior of the cross flow mechanical draught cooling tower in south Tunisia conditions leads to conclude results serving to understand the operation conditions of the system. The analysis of the distribution of air and water temperatures highlights the phenomenon of negative convection inside the tower. At a given height of the tower, water temperature becomes lower than the one of air and the two fluids are simultaneously cooled.

The study of the heat and mass exchanges processes inside the cooling tower shows that the water cooling is performed mainly by evaporation potential compared to the convective one.

The water loss by evaporation represents about 5.1% of the total water quantity feeding the cooling tower; the cumulative quantity during one year was estimated by $1.8 \cdot 10^6 \text{ m}^3$. This represents the yearly domestic water consumption of about 90,000 inhabitants. Further investigations should be carried in the future to find solutions in order to recover these quantities of evaporated water.

REFERENCES

- Ayoub, J., and Alward, R.: Water requirements and remote arid areas: the need for small-scale desalination, Desalination, 107, (1996), 131-147.
- Bernier, M.A.: Cooling tower performance: theory and experiments, ASHRAE Trans, 100, (1994), 114-121.
- Bernier, M.A.: Thermal performance of cooling towers, ASHRAE Journal of transfer, 7, (1995), 56-61.
- Braun, J.E., Klein, S.A., and Mitchell, J.W.: Effectiveness models for cooling towers and cooling coils, ASHRAE Tans, 95, 2, (1989), 164-174
- El-Dessouky, H.T.A., Al-Haddad, A., and Al-Juwayhel, F.: A modified analysis of counter flow cooling towers, ASME Journal of Heat Transfer, 119, 3, (1997), 617-626
- Halasz, B.: A general mathematical model of evaporative cooling devices, Revue Générale de Thermique, 37, (1998), 245-255.
- Jaber, H., and Webb, R.L.: Design of cooling towers by the effectiveness-NTU method, ASME Journal of Heat Transfer, 119, 3, (1997), 617-626.
- Kairouani, L., Hassairi, M., and Zermani, T.: Performance of cooling tower in south of Tunisia, Building and Environment, 39, pp (2004), 351-355.
- Merkel, F.: Evaporation-Refrigeration, J. Assoc. German Eng., 70, (1925), 123-131
- Milosavljevic, N., and Heikkilä, P.: A comprehensive approach to cooling tower design, Applied Thermal Engineering, 21, (2001) 899-915.

Walker, W.H., Lewis, W.K., and McAdams, W.H.:
Principles of chemical engineering. McGraw-Hill, New
York. (1923)